applied sciences

MDPI

Article

Designing and Manufacturing an Affordable and Easy to Use Visual Bio Feedback Device to Fix Forward Head Posture: A Pilot Study Involving Female Students

Mehran Emadi Andani [1,*], Bahar Lotfalian [2] and Ata Jahangir Moshayedi [3,*]

[1] Department of Neurosciences, Biomedicine and Movement Sciences, University of Verona, Via Casorati, 37131 Verona, Italy
[2] Department of Biomedical Engineering, Ragheb Esfahani Institute of Higher Education, Isfahan 8436113131, Iran; bahlotfalian@gmail.com
[3] School of Information Engineering, Jiangxi University of Science and Technology, Ganzhou 341000, China
* Correspondence: mehran.emadiandani@univr.it (M.E.A.); ajm@jxust.edu.cn (A.J.M.)

Abstract: Forward Head Posture (FHP) is when the head leans forward due to factors such as heavy backpacks or poor computer ergonomics. FHP can lead to neck strain and discomfort as well as potential long-term issues such as arthritis. Treatment options include specialized exercises, orthopedic devices, manual therapy, physical exercises, and visual feedback techniques, along with guidance from specialists in physical medicine and rehabilitation. In this study, a visual feedback-based approach was used to address FHP in female students. The study spanned ten days and included a visual feedback group and a control group. The results showed significant improvements in maximum head angle deviation in the visual feedback group compared to the control group; however, there was no significant change in the DFA number, indicating stability in policy control by the central nervous system. The study demonstrated that visual feedback sessions led to immediate benefits, with participants progressively acquiring skills involving the maintenance of proper head positioning. The test results indicated that the neck angle decreased to less than 15 degrees, indicating a return to a normal state. The versatility of the developed affordable and easy-to-use device and the potential for using smartphone motion sensors for similar visual feedback systems are discussed in this paper as well. The study suggests the promising potential of visual feedback in healthcare, including remote monitoring and smartphone-based solutions.

Keywords: forward head posture; visual feedback; bio-feedback; Arduino UNO; 3D accelerometer; healthcare

Citation: Emadi Andani, M.; Lotfalian, B.; Moshayedi, A.J. Designing and Manufacturing an Affordable and Easy to Use Visual Bio Feedback Device to Fix Forward Head Posture: A Pilot Study Involving Female Students. *Appl. Sci.* **2024**, *14*, 781. https://doi.org/10.3390/app14020781

Academic Editor: Marius Baranauskas and Rimantas Stukas

Received: 5 November 2023
Revised: 5 January 2024
Accepted: 5 January 2024
Published: 17 January 2024

1. Introduction

One of the prevailing issues concerning bodily posture pertains to the phenomenon of Forward Head Posture (FHP). FHP is a condition characterized by the forward positioning of the head in relation to the shoulders and spine. In light of the predominant nature of human interaction occurring anteriorly vis-à-vis the countenance, protracted engagements with computer usage, television consumption, video game indulgence, unforeseen mishaps, or the protracted carriage of backpacks have been identified as potential antecedents to the proclivity of cranial inclination towards the anterior plane [1].

1.1. FHP Reasons and Causes

In the broad spectrum of causative elements contributing to this phenomenon, a succinct enumeration of pivotal determinants is presented in the following sections: Backpack Overloading [2], Computer Utilization Ergonomics [3], Traumatic Incidents [4], Ocular Impairment [5], and Ambulation Anomalies [6]. Notably, this constellation of secondary effects encompasses an array of deleterious consequences, including but not limited to those delineated in Figure 1.

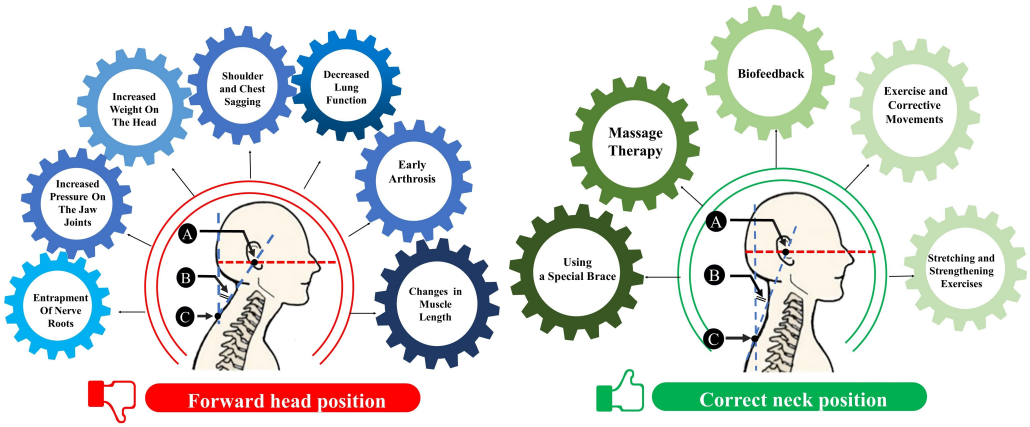

Figure 1. Comparing forward head (red) and correct head (green) positions: A, Tragus; B, α (Head/Neck angle); C, C7 (seventh cervical vertebra).

In an optimal scenario, the cranial region should be impeccably aligned with the cervical and scapular regions, akin to the harmonious equilibrium of a golf ball atop its pedestal. In stark contrast, the human cranium presents a significantly heftier mass, more akin to that of a bowling ball; consequently, the anterior inclination of the head imposes a substantial biomechanical strain on the cervical and dorsal musculature. It is noteworthy that the gravitational burden on the cervical spine escalates for every increment of the anterior displacement of the cranium, as reported in Table 1 [7].

Table 1. Intensity of pressure on the neck in different neck angular positions.

Neck Angular Position	Intensity of Pressure in the Neck (kg)
4–5	Head in normal position
12	Head forward α =15 degrees
18	Head forward α = 30 degrees
22	Head forward α = 45 degrees
27	Head forward α = 60 degrees

As delineated in Table 1, each increment of 15 degrees in the anterior displacement of the head imposes an excessive load akin to the initial pressure upon the cervical region [7].

Consequently, this increased pressure engenders cervical weariness and concomitant persistent or predominant cervical discomfort. The musculature spanning the cervical and scapular regions is entrusted with the perpetual sustenance of this burdensome load, and sustains an isometric contraction, culminating in hemodynamic impairment, tissue trauma, and exhaustion ultimately manifesting as elongation, soreness, a burning sensation, and fibromyalgia [8]. Furthermore, the anterior inclination of the head and neck precipitates the erasure of the inherent cervical lordosis, thereby compromising the integrity of the intervertebral discs and potentially fostering premature arthritic degeneration [9].

1.2. Treatment Modalities and Strategies

The initial phase of addressing ailments related to the head and neck necessitates thorough evaluation by a specialist in physical medicine and rehabilitation complemented by radiographic assessments to gauge the progression of the condition. Subsequent to this comprehensive assessment, a tailored treatment regimen is prescribed encompassing specialized exercises and an array of therapeutic interventions. Several therapeutic modalities warrant consideration, including stretching and strengthening regimens, offered by a physical medicine and rehabilitation specialist as a series of exercises [10], utilization of a bespoke orthopedic apparatus such as an orthopedic device (e.g., braces or lumbar supports) designed to facilitate optimal bodily posture [11], manual techniques such as the application of massage therapy [12], structured physical exercises or corrective movements [13,14], and

biofeedback techniques such as therapeutic–educational modalities wherein individuals are instructed on the volitional regulation of innate autonomic physiological functions to influence overall bodily wellbeing [15].

2. Related Works

Biofeedback, in its canonical manifestation, emerges as a therapeutic method underpinned by the sophisticated apparatus of modern electronics, serving as a conduit for the comprehensive measurement and intricate analysis of the multifarious neural, muscular, and autonomic processes inherent to the human corpus [16]. These invaluable insights gleaned from the depths of biofeedback instrumentation are subsequently imparted to the patient and their medical practitioner(s) through the medium of auditory or visual feedback, culminating in a symbiotic dyad of informed collaboration [17–19]. For patients, the biofeedback apparatus functions as a quasi-sensorial adjunct, affording them the rarefied capacity to perceive and cognize the inner workings of their corporeal vessel [20]. In a notable example, someone using a blood pressure monitor can actually lower their own blood pressure by simply concentrating on the screen [21]. When acquiring skills such as biking, driving, or sports, this unspoken skill of blood pressure control combines mental and physical aspects. It is developed through trial and error, hands-on learning, and dedicated practice [22]. Biofeedback equipment translates physiological signals into audio–visual feedback, aiding in the treatment of various conditions including neurological and muscular issues, tension-related problems, and gastrointestinal disorders [23]. These devices are temporary tools for learning and experimentation, becoming unnecessary when proficiency is attained. Biofeedback is particularly effective in cases where pharmaceutical interventions fall short [24].

A recent paper [25] introduced a biofeedback system using an accelerometer. In a five-hour study with six participants, the authors found that the system significantly reduced time spent in poor posture. The biofeedback system interfaced with a computer and provided real-time feedback on the user's neck angle through a visual display and auditory cues. While initial sessions recorded neck movements without feedback, subsequent sessions with active biofeedback showed improved posture. It is worth noting that continuous use of the biofeedback system was required in order to maintain good posture, and there was no information on lasting effects after the study.

In [26], researchers introduced an innovative biofeedback system with a camera on a computer monitor, auditory cues, and a tactile feedback necklace. Participants read on their computers with the option of using auditory or tactile feedback. Results showed improved neck angles with both feedback methods, and there was a significant change in neck angle even without feedback. While this study demonstrated the rapid effectiveness of biofeedback within a single 90-min session, the long-term benefits remain uncertain. In [27], the authors suggested that individuals can learn to improve their head and neck posture through the use of a biofeedback system. The system continuously monitors head and neck alignment, providing real-time feedback through a smartphone app. It uses signals such as sounds, music, vibrations, and flashes to warn users about poor posture. Data collected are securely stored and can be shared with healthcare professionals; however, the device does not quantify the extent of posture improvement, highlighting the need for web services to access comprehensive data.

In another study, [28] used neurofeedback to improve neck posture in individuals with forward head syndrome. Participants were split into two groups, one receiving neurofeedback training and the other acting as a control. Both groups underwent a four-week, thrice-weekly program that included unique activities such as pottery and brainwave-controlled archery to enhance concentration. After the training, the neurofeedback group showed significant improvements in neck mobility, as documented through post-training assessments.

In [29], a study was conducted in which participants performed a one-hour typing task twice, once with biofeedback and once without. The researchers attached the biofeedback

device to the participants and instructed them on maintaining an upright posture. Using motion analysis and discomfort assessments, this study found that the biofeedback device significantly improved the posture of individuals experiencing neck discomfort during computer-related tasks. Forward head posture is a common issue with potential health risks, and various treatments have been explored. Common biofeedback methods are reviewed in Table 2, although biofeedback can refer to other devices as well [30,31].

Table 2. Biofeedback methods and principle.

Method	Principle
Surface Electromyography (sEMG)	Measures muscle activity in the neck and upper back, offering feedback on muscle activation during poor posture [32].
Pressure Biofeedback	Utilizes a device under the neck or upper back to measure pressure changes, aiding in teaching individuals how to maintain proper posture [33].
Wearable Posture Sensors	Devices such as posture correctors or sensors provide real-time alerts or reminders when users deviate from correct posture, encouraging better habits [34].
Visual Feedback Systems	Mirrors, video monitoring, or software applications offer visual cues about current posture, allowing users to adjust and correct their alignment [35].
Auditory Feedback Devices	Devices produce sounds or alerts when posture deviates, serving as a reminder to adjust and maintain proper alignment [36].
Virtual Reality (VR) Augmented Reality (AR)	Postures is simulated to provide interactive feedback in order to help individuals learn to correct their forward head posture [37].

In terms of performance, according to the Table 2, advanced sEMG and VR/AR methods provide more complete feedback but are less accessible due to their complexity. On the other hand, wearable sensors and visual and auditory feedback devices have slightly different performance, are more accessible, and are more popular while requiring less specific settings [38].

With respect to the aforementioned biofeedback types and reviewed papers, the present research highlights the benefits of biofeedback treatment, which is cost-effective, has a shorter treatment duration, and has minimal side effects compared to other methods.

In the context of the current research endeavor, the objectives are multifaceted and pioneering. The core aim of this research centers on the development of a system which, for the first time, harnesses accelerometer sensors to comprehensively characterize neck behavior. In the field of healthcare, the development of cost-effective and user-friendly medical devices constitutes a significant and imperative concern [39,40]. This system, seamlessly integrated with the MATLAB program's graphical user interface, serves the purpose of visually rendering neck behavior to the individual. This pioneering research thereby represents a pivotal step forward in harnessing biofeedback methodologies to address anatomical issues and empower individuals to actively participate in the amelioration of their health and wellbeing. This study focuses on the efficacy of biofeedback treatment, highlighting its distinct advantages over alternative methods. Biofeedback therapy stands out due to its cost effectiveness, short and effective treatment, and absence of adverse effects on patients. In this endeavor, we aim to address the following objectives:

1. Apply biofeedback (visual feedback) techniques in an innovative manner to address anatomical issues related to the cervical vertebrae.

2. Develop a pioneering system that utilizes accelerometer sensors to comprehensively characterize neck angular behavior.
3. Seamlessly integrate the developed system with the MATLAB program's graphical interface.
4. Provide individuals with a visual representation of their neck behavior to enhance awareness.
5. Enable individuals to observe and gain awareness of maladaptive neck positioning.
6. Foster a pathway for self-correction of neck angle anomalies.
7. Empower individuals to actively participate in improving their health and wellbeing through visual feedback methodologies.

The paper is organized as follows: Section 3 introduces the designed device, offering in-depth details about its specifications and features; Section 4 presents the results; finally, the concluding section provides a summary of the key findings and conclusions drawn from this research.

3. Materials and Method

3.1. Participants

A prior sample size calculation was performed using G-Power 3.1 [41] for the F-test, utilizing the repeated measures method of interactions. Based on an effect size of 0.25 (considered an average size according to [42]), an α error probability of 0.05, a desired power (β—1 error probability) of 0.95, ten measurements taken over a span of 10 days, a correlation of 0.5 between repeated measurements, and a non-spherical correction parameter ϵ of 1, the calculated sample size was 10 for each group. To mitigate potential data loss, we decided to include 15 participants for each group. The study involved female students from Farzangan Amin High School in Isfahan, Iran. The participants had an age range of 16.5 to 17.6 years, with an average age of 16.9 ± 0.5 years. All participants were diagnosed with a forward head problem with no history of other medical conditions or musculoskeletal issues. The two VF and control groups were not different in terms of age, body height, or body weight ($p > 0.284$). Prior to participation, written consent was obtained from all students, as documented in the references.

3.2. Hardware

The two core components of the system, i.e., hardware and software, are illustrated in Figure 2. The hardware segment encompasses an ADXL345 accelerometer and an Arduino UNO micro-controller serving as the central processing unit. Conversely, within the software realm, MATLAB is harnessed for the presentation and analysis of the acquired data. The ADXL345 accelerometer sensor is utilized to gauge neck angles, while the Arduino UNO micro-controller interface is responsible for capturing accelerometer data and transmitting it to the computer. In the software domain, MATLAB assumes a dual role: (a) providing real-time data visualization on the monitor, represented as a red circle, and (b) registering signals to facilitate subsequent data processing. The Arduino UNO is a popular micro-controller board featuring an AT-mega328P processor running at 16 MHz. It offers 32 KB of flash memory for program storage and 2 KB of SRAM for data. The board has 14 digital input/output pins, 6 analog inputs, and supports PWM [43].

The ADXL345 is a digital accelerometer sensor by Analog Devices, boasting good versatility. It can measure acceleration in three axes (x, y, and z) with a resolution of up to 13 bits [44]. To calculate the parameters using the accelerometer, the angle of deviation from the central state is determined in degrees using Equation (1):

$$\text{Angle} = \cos^{-1}\left(\frac{x \cdot x_{0+} y \cdot y_{0+} z \cdot z_0}{\sqrt{x_0^2 + y_0^2 + z_0^2} \cdot \sqrt{x^2 + y^2 + z^2}}\right) \quad (1)$$

where x_0, y_0, and z_0 are the coordinates of the initial orientation of the head, while x, y, and z are the current orientation of the head during the experiment.

3.3. Software

As mentioned, the software used in this study was MATLAB. The written code's functionalities are as follows. Initialization Step: the program commences by establishing a serial port (COM6 in our computer) through the 'serial' command, operating at a bit transfer rate of 115,200 bits per second. Subsequently, the Arduino data file is opened using the 'fopen' command, enabling data retrieval.

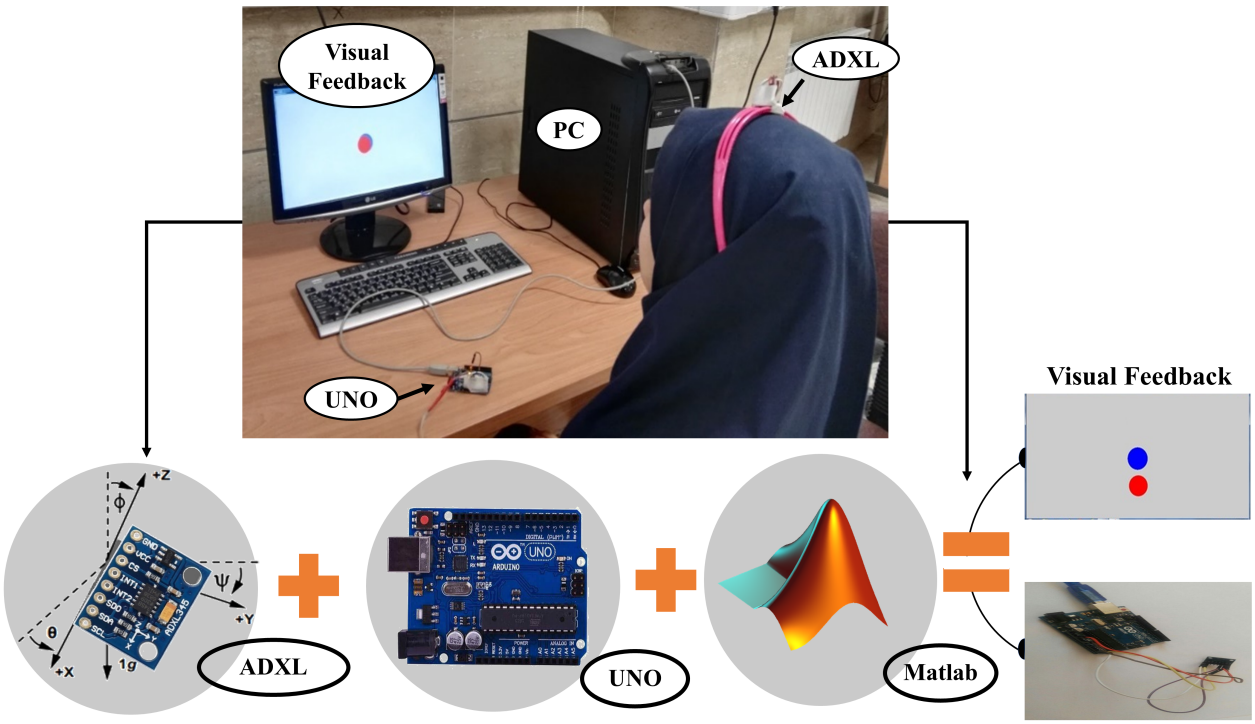

Figure 2. Experimental setup: the experimental setup, including accelerometer (ADXL345) mounted on the head of the subject, Arduino UNO, MATLAB, and PC, is illustrated in this figure.

- Data Acquisition: data from the Arduino are read from the file using the 'fscanf' command. The program defines parameters related to the accelerometer sensor, including 'MaxValue', 'Resolution', 'Fs' (sampling frequency), and 'MaxAcc_g'.
- Data Storage Loop: a loop is established to collect accelerometer sensor values, specifically, the acceleration values in the Earth's gravity direction (x, y, and z axes); these values are stored in the 'xyz' variable over a period of 120 s.
- Visualization Step: the program employs the 'plot' command to draw a blue circle at the center of the monitor screen to serve as a reference point, and maintains it on the screen using the 'hold on' command.
- Angle Calculation: the accelerometer sensor supplies data regarding the Earth's gravitational acceleration in the x, y, and z directions. Using these values, the program computes the head's angle for both forward and backward bending as well as left and right bending directions using Equations (2) and (3), respectively.

$$\theta = \tan^{-1}\left(\frac{A_x}{\sqrt{A_y^2 + A_z^2}}\right) \tag{2}$$

$$\psi = \tan^{-1}\left(\frac{A_y}{\sqrt{A_x^2 + A_z^2}}\right) \tag{3}$$

The real-time position of the sensor is visually represented by a red circle on the same page. The sampling rate was set at 100 Hz. Following resampling, the data are subjected to a

10 Hz low-pass filter to reduce noise. Finally, the program generates visual representations of the sensor's movements. As depicted in Figure 2, the ADXL345 accelerometer sensor is firmly affixed to a plastic holder to eliminate unintended movements. Subsequently, it is connected to the Arduino UNO board using the appropriate protocol connectors. The Arduino board is further connected to a computer or laptop through the USB port. When the sensor is positioned on the individual's head, the data related to head angle are transmitted via the board to the MATLAB software running on the computer. The individual is then guided to adjust their head position based on the displayed angle information.

3.4. Data Collection and Protocol

As depicted in Figure 3, the accelerometer sensor was meticulously affixed to a plastic holder and securely adhered in place through the judicious application of adhesive. Pertinent to the experimental configuration, certain parameters merit attention. Participants sat on a comfortable chair in front of a monitor. The participant's cranium was established at a distance of 80 cm. This interplay of measurements contributed to the precision and integrity of the experimental environment, offering a robust foundation for data acquisition and analysis. An expert set the correct position of the head and neck soon before starting each experimental session [45]. In the ensuing interlude, denoted as the second phase, the participant was granted a respite, affording them the freedom to move their head while remaining seated in the chair and permitting relaxation without specific posture constraints. The third phase (session 2) introduced visual feedback into the participants in the VF group. They were required to adopt an upright seated position, concomitantly positioning the sensor on their cranium while meticulously aligning their head in the prescribed orientation. Notably, the monitor was activated during this phase, ushering in real-time feedback. Data acquisition commenced under these monitored conditions, as delineated in Figure 3. It should be mentioned that for the participants in the control group there was no visual feedback, and the session was identical to session 1. The experimental protocol unfolded in a structured sequence comprising distinct phases. These procedural steps were meticulously designed to investigate the impact of visual feedback on posture maintenance. Each phase endured for a duration of two minutes, fostering comprehensive data acquisition and assessment. The inaugural phase, conducted without visual feedback, beckoned the participant to assume a proper seated posture. Ensuring precision, the sensor was affixed to the individual's cranium while meticulously anchored to its holder, nullifying any unintended displacement. The head assumed its ideal position, albeit slightly offset from the habitual stance, due to the presence of forward head syndrome. Subsequently, the participants were instructed to maintain this posture with the monitor deactivated, enabling discreet data recording.

A subsequent intermission, designated as the fourth phase, allowed the participants to again enjoy a brief respite wherein they retained the liberty to move their head while maintaining a seated position. The fifth and final phase (Session 3), mirroring the initial phase but was conducted without visual feedback, compelling the participants to sit upright. The sensor iwass again situated on the cranium and with the head meticulously aligned. However, in this instance the monitor remained inactive, and data recording was resumed under these circumstances. It is worth noting that these test procedures were iteratively administered across ten sessions for each participant to ensure the robustness and reliability of the data collection process. For visual feedback, during the third phase of the experiment (Session 2), the experimenter orchestrated the alignment of the subject's head into an optimal orientation, with subsequent instructions to sustain this posture. Importantly, this phase entailed the activation of the monitor with visual display. The display featured a centrally positioned stationary blue circle alongside a dynamically mobile red circle representing the real-time tracking of the subject's head position. The subject was explicitly directed to superimpose the mobile red circle onto the stationary blue circle, thereby perpetuating a state of alignment between their head position and the designated reference point. This technologically mediated mechanism leverages visual

feedback, facilitating the subject's acquisition of the requisite skills to consistently maintain their head in the correct position, as illustrated in Figure 4.

Figure 3. Experimental protocol. The experiment contained three experimental sessions with two interval rests. The first and last sessions were identical for both groups. Moreover, the second session of the control group was similar to the other sessions. However, in the second session of the VF group, visual feedback was provided for the participants to help them keep their heads in the correct position.

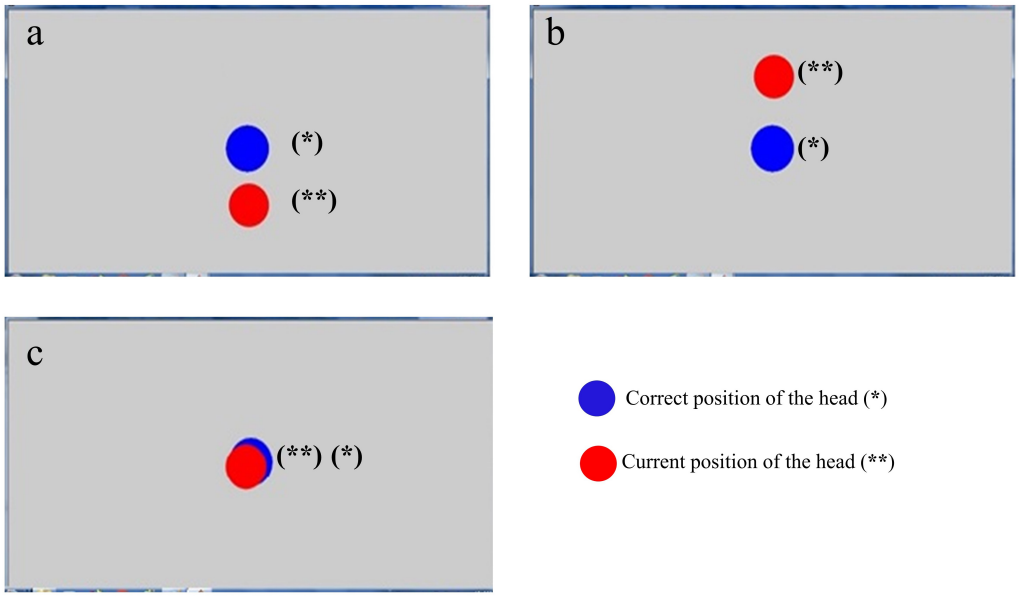

Figure 4. A view of the monitor during the execution of the program in the third phase of the experiment. The blue circle is the reference in the middle of the screen and shows the proper position of the head, while the red circle shows the instantaneous position of the head: (**a**) when the head is behind the proper position, (**b**) when the head is ahead of the proper position, and (**c**) when the head is in the right position. The red circle can appear on the right or left side of the blue circle to indicate the head's inclination to the right or left side, respectively.

We utilized the ADXL345, a 3D accelerometer sensor capable of determining the angular position relative to the gravity vector. This position was employed to offer visual feedback to participants, as detailed in Figure 4. As illustrated, the red circle moves above or below the blue circle if the head tilts forward or backward, respectively. Similarly, if the head tilts left or right this causes the red circle to shift to the corresponding side of the blue circle. Thus, the red circle's position on the PC monitor corresponds linearly to the angular head position. Notably, the blue circle remains fixed at the center of the PC monitor as a reference point.

3.5. Metrics

Within the purview of this investigation, an array of parameters underwent rigorous scrutiny, encompassing the following: maximum head angle deviation, effective range of head angle deviation (i.e., movement variability), and the Detrended Fluctuation Analysis (DFA) number. To commence, the angular deviation from the central position was meticulously quantified in degrees. The maximum magnitude among these calculated values was ascribed as the pinnacle of head angle deviation, while the arithmetic mean thereof was used to represent the average deviation of the head angle. Notably, the standard deviation within each registration affords insight into the amplitude of fluctuation characterizing the head angle deviation, thereby delineating its effective range. Furthermore, the DFA coefficient, elaborated upon in a subsequent section, was computed for each registration, adding an additional layer of complexity to the analytical framework.

DFA Number

Drawing inspiration from the intricate fractal patterns arising from the juxtaposition of repetitive motifs, time series data can be scrutinized through a fractal lens. Within the framework of the DFA method, these fluctuations are conceptualized as a metric gauging randomness [46,47]. By assessing the degree of randomness inherent in these fluctuations, the DFA method effectively quantifies the self-similarity embedded within the recorded time series. The fundamental underpinning of this method bears a resemblance to the root mean square error, distinguished by its superior resilience to the nonstationarity inherent in the examined processes [48]. Equation (4) furnishes the means to calculate the extent of fluctuations.

$$F(n) = \sqrt{\frac{1}{N}\sum_{k=1}^{N}[y(k) - y_n(k)]^2} \tag{4}$$

Here, the variable $y(k)$ denotes the integral of the analyzed time series, spanning a length of N, which is partitioned into sub-intervals of variable length n. The selection of 'n' is contingent upon the temporal span of the time series and the periodicity of embedded patterns, yielding diverse potential values. Concurrently, $y_n(k)$ denotes the coefficients associated with the gradient of the least-squares error line, customarily fitted to each respective sub-interval. An exploration of the relationship between $F(n)$ and 'n' illuminates a notable exponential growth in the magnitude of fluctuations as the sub-interval length expands. Remarkably, this relationship exhibits near-linearity within the log–log framework. Specifically, $F(n)$, which quantifies the extent of fluctuations, is effectively approximated by n^{α}. The parameter 'α', commonly referred to as the DFA number, represents the slope of the tangent line on the log–log graph correlating $F(n)$ and 'n'. This crucial parameter substantiates the extent of correlation among fluctuations. The interplay between α and the stochastic nature of temporal variations across the successive phases is succinctly encapsulated within the confines of Equation (7).

$$\alpha < 0.5 \quad \text{Negative correlation} \tag{5}$$

$$\alpha = 0.5 \quad \text{Zero correlation} \tag{6}$$

$$\alpha > 0.5 \quad \text{Positive correlation–Completely random} \tag{7}$$

The outcomes derived from this methodology serve a dual role, finding utility in the realm of biological elucidation of motor control dynamics [49]. Notably, a key advantage inherent in the application of this method lies in its capacity to provide substantiation for the underlying biological architecture of the central nervous system. For instance, the findings gleaned through this approach have been correlated with the intricate network of supra-spinal circuits implicated in motor control. Furthermore, the attained results furnish valuable insights into the operational mechanics of the central pattern generator responsible for orchestrating rhythmic motor movements.

3.6. Statistical Analysis and Results

Through the application of the bespoke system developed for this study, continuous monitoring and computation of the head angle in relation to its initial positioning were conducted in real-time. Within each 2-min recording session, four distinct metrics were systematically derived to assess each individual's performance across multiple sessions and days, encompassing evaluations before, during, and after feedback. Among these metrics, paramount attention was directed to the maximal computed value, representing the zenith of head angle deviation from its initial alignment. Simultaneously, the arithmetic mean of these values was computed to provide an overview of the average head angle deviation. Furthermore, meticulous calculation of the standard deviation was performed for each recording, serving as a pivotal statistical measure that conveyed the effective amplitude governing fluctuations in head angle deviation. In concert with these parameters, the calculation of the DFA number was undertaken during each recording, contributing to a comprehensive evaluation of performance and responsiveness within the experimental paradigm.

4. Results

4.1. Maximum Head Angle Deviation

The maximum head angle deviation is illustrated across ten days, contrasting the states preceding feedback, concurrent with feedback, and subsequent to feedback in the VF group and three sessions without visual feedback in the control group as it shown in Figure 5.

Additionally, to provide a better picture for comparison of the two groups, the results are illustrated in Figure 6. The figure provides a comparative visualization of the maximum head angle deviation between the two groups on different days. Similarly, the two groups are illustrated on Figure 7 to compare sessions within groups.

An analysis of variance (ANOVA) conducted on the maximum head angle deviation revealed a significant effect of the Day because of the higher values on day 1 compared to the other days ($F(9,252) = 11.33$, $p < 0.001$, $np^2 = 0.288$, Session ($F(2,56) = 46.47$, $p < 0.001$, $np^2 = 0.624$) because of the higher values on session 1 compared to sessions 2 and 3 as well as of the Group because of the lower values in the VF group compared to the control group ($F(1,28) = 88.42$, $p < 0.001$, $np^2 = 0.759$). Moreover, the Day × Session × Group interaction was significant ($F(18,504) = 3.06$, $p < 0.001$, $np^2 = 0.098$).

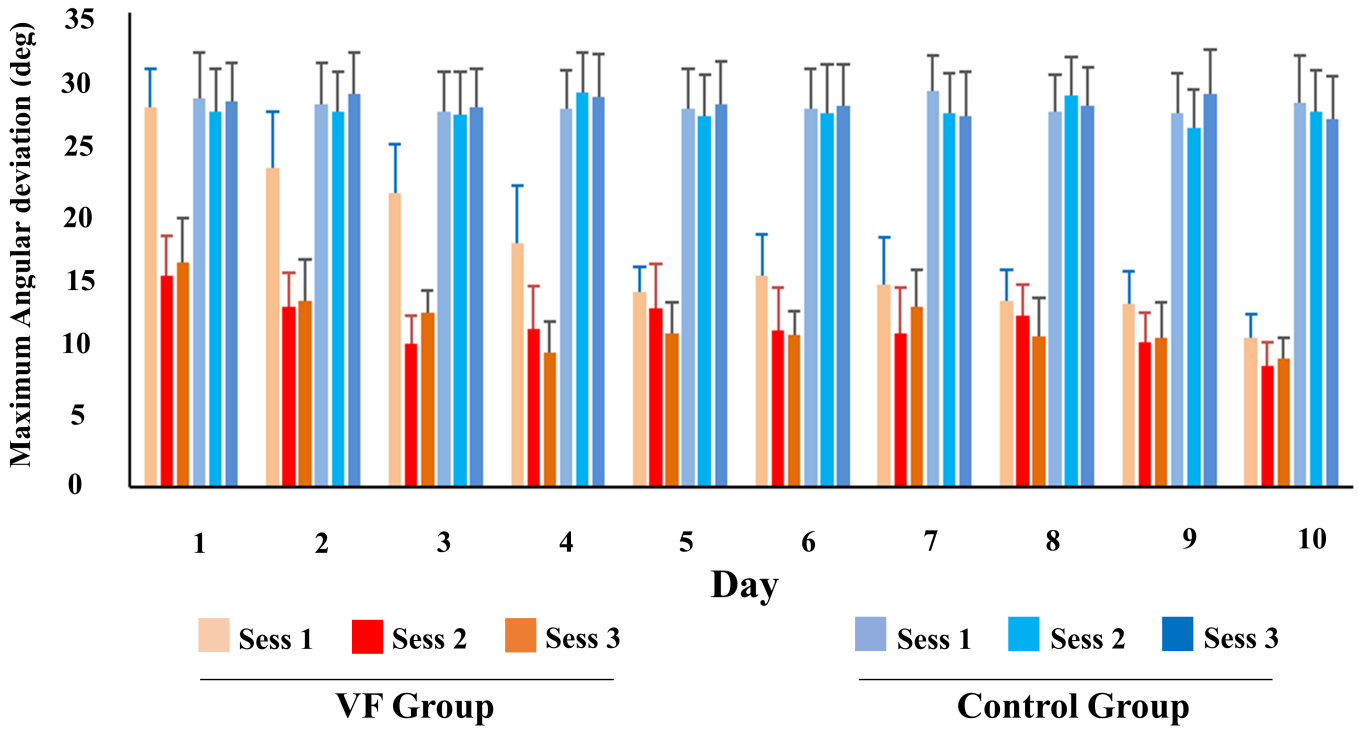

Figure 5. Maximum angular deviation of the head. The data for the VF and control groups are presented over a ten-day period. The data are represented in three sessions: Sess. 1, Sess. 2, and Sess. 3. The values are expressed as mean values with corresponding standard errors.

As shown in Table 3, post hoc analysis revealed a significant difference between the VF and control groups on each day during sessions 2 and 3 as well as on days after the third during session 1 ($p < 0.009$, Cohen's d > 0.73; Figure 6). Only on days 1 and 2 was there no difference between groups during session 1 ($p > 0.066$). It can be confirmed that the visual feedback has a strong effect on decreasing the values and that this effect was consolidated across days. Moreover, the results confirm that in the VF group there was a significant reduction in sessions 2 and 3 compared to session 1 on days 1 to 5 ($p < 0.046$, Cohen's d > 0.67). Instead, on days 6 and after, there was no difference between the three sessions in the VF group ($p > 0.141$). In the control group, there was no difference between sessions on each day ($p > 0.848$).

Table 3. Maximum angular deviation of the head. The data for the VF and control groups are presented over a ten-day period. The data are represented in three sessions (Sess. 1, Sess. 2, and Sess. 3). The values are expressed as mean values ± standard errors.

Day	VF Group			Control Group		
	Session 1	Session 2	Session 3	Session 1	Session 2	Session 3
1	28.11 ± 2.76	15.57 ± 3.02	16.56 ± 3.30	28.97 ± 3.36	27.39 ± 2.78	27.72 ± 3.56
2	23.57 ± 4.16	13.30 ± 2.51	13.79 ± 3.02	27.86 ± 3.04	28.54 ± 2.99	28.20 ± 3.52
3	21.77 ± 3.60	10.57 ± 2.07	12.85 ± 1.68	28.40 ± 3.12	28.01 ± 2.74	28.54 ± 3.04
4	17.99 ± 4.25	11.71 ± 3.14	9.89 ± 2.29	28.42 ± 2.99	28.56 ± 2.88	27.68 ± 2.80
5	14.41 ± 1.80	13.20 ± 3.28	11.38 ± 2.29	27.69 ± 3.34	27.90 ± 2.78	29.27 ± 2.83
6	15.60 ± 3.04	11.55 ± 3.19	11.26 ± 1.74	28.24 ± 3.21	27.60 ± 3.14	28.15 ± 2.82
7	14.91 ± 3.49	11.38 ± 3.30	13.34 ± 2.69	29.08 ± 2.91	27.26 ± 2.96	27.46 ± 3.70
8	13.73 ± 2.29	12.64 ± 2.26	11.12 ± 2.81	28.60 ± 2.74	28.66 ± 3.28	27.44 ± 2.91

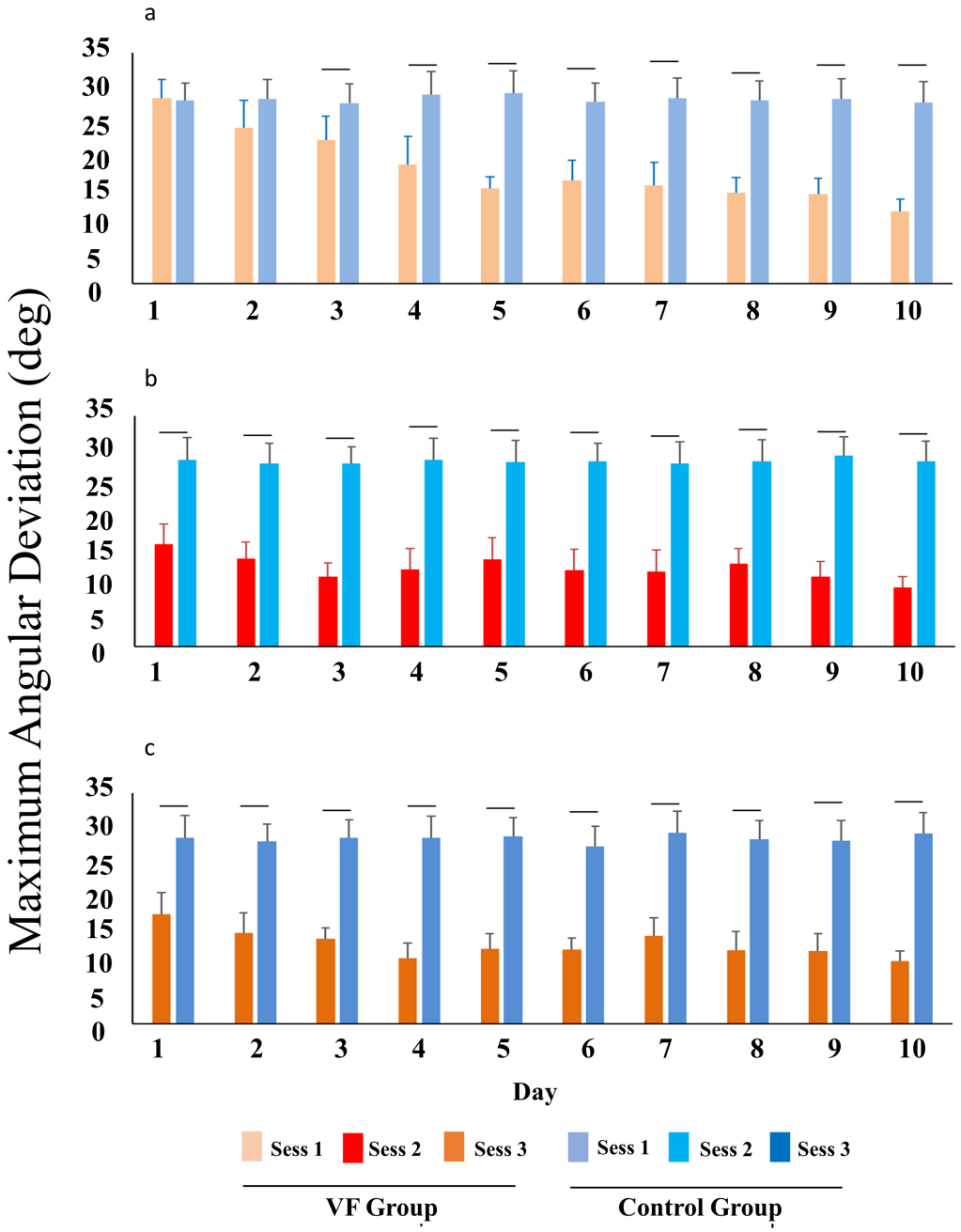

Figure 6. Maximum angular deviation of the head; the data for the VF and control groups are presented over a ten-day period. The data are represented in three sessions: Sess. 1 (**a**), Sess. 2 (**b**), and Sess. 3 (**c**). The values are expressed as mean values with corresponding standard errors. The horizontal black lines represent the significant difference between groups. The level of significance is set at $p < 0.05$.

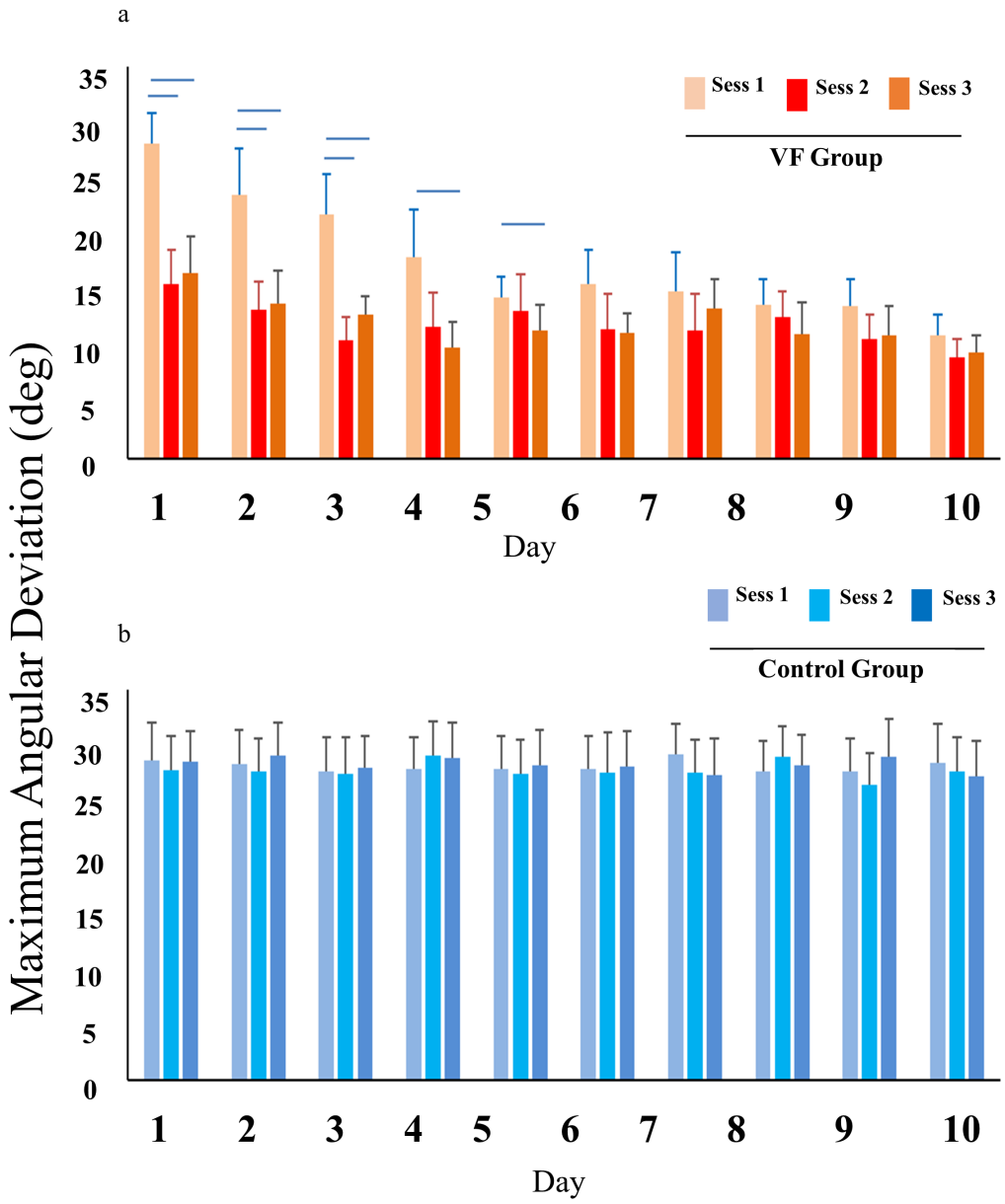

Figure 7. Maximum angular deviation of the head. The data are presented over a ten-day period for the VF (**a**) and control (**b**) groups. The data are represented in three sessions: Sess. 1, Sess. 2, and Sess. 3. The values are expressed as mean values with corresponding standard errors. The horizental black lines represent the significant difference between sessions. The level of significance is set at $p < 0.05$.

4.2. DFA Number

Figure 8 provides a graphical depiction of the DFA number across ten distinct days, notably segregated into the three sessions of the two groups VF and control). ANOVA analysis revealed that there were no statistically significant effects of the Day, Session, Group, or their interactions ($p > 0.272$). This absence of statistical significance underscores the constancy and consistency of DFA numbers over the course of the study.

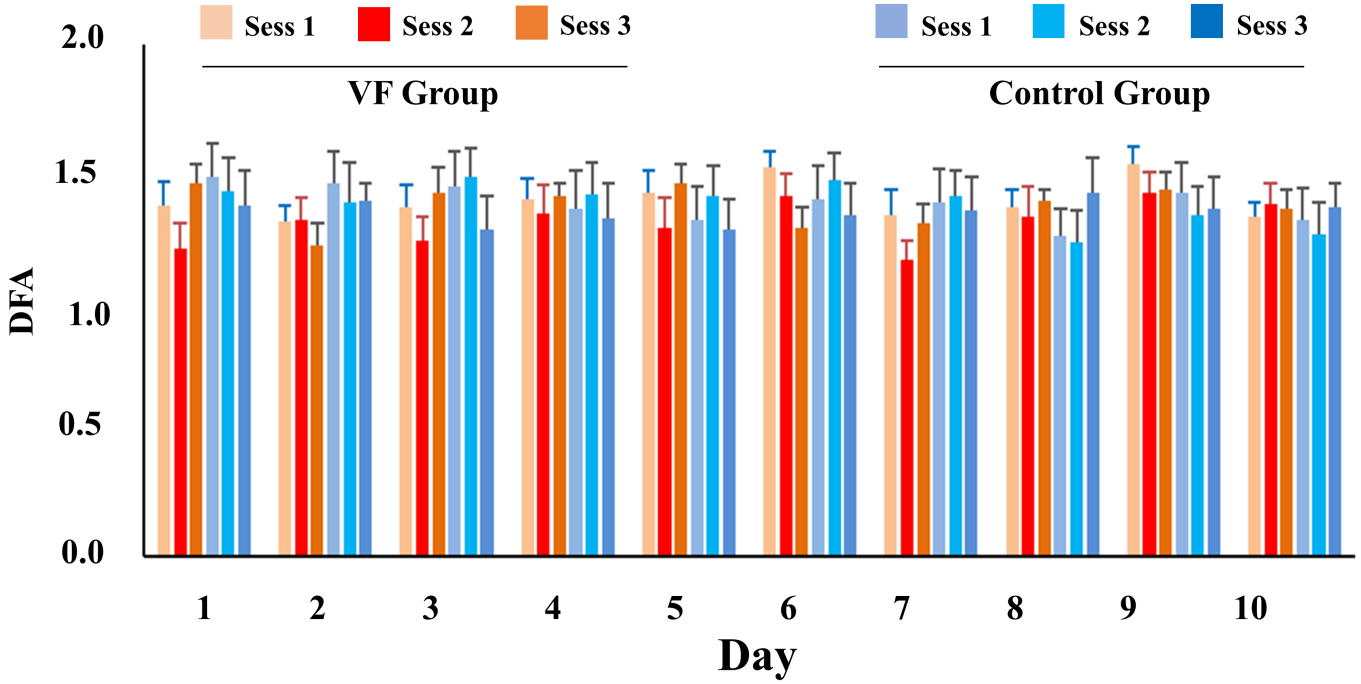

Figure 8. DFA number; the data for the VF and control groups are presented over a ten-day period. The data are represented in three sessions: Sess. 1, Sess. 2, and Sess. 3. The values are expressed as mean values with corresponding standard errors.

5. Conclusions and Suggestions

Within this empirical investigation, a visual feedback-based apparatus was meticulously devised to address the persistent issue of forward-facing head orientation and the ensuing afflictions encompassing head and neck discomfort. By enabling female students to observe and cognitively engage with the dynamics of their neck behavior, the participants acquired the ability to rectify this maladaptive conduct, culminating in amelioration of the neck angle and proper repositioning of the head. The study results show how a visual feedback tool can effectively correct head posture in female students. Future research might consider incorporating audio cues in a headset linked to the sensor for easier use in everyday life. These findings underscore the tool's potential for posture correction and ways to make it more practical in healthcare settings.

Notably, all three metrics, comprising the maximum head angle deviation, the average head angle deviation, and the effective amplitude of head angle deviation, exhibited a marked and statistically significant enhancement on the tenth day vis-à-vis the inaugural day.

Remarkably, the values of these indicators preceding the feedback sessions on the tenth day registered a discernibly diminished magnitude when juxtaposed with their corresponding values prior to feedback initiation on the first day. Furthermore, the results underscored that the aforementioned indicators post-feedback on the tenth day exhibited a notably diminished magnitude when contrasted with their antecedent counterparts preceding the feedback on the first day. After a 10-day test duration, the results indicated that the neck angle decreased to less than 15 degrees, signifying a return to a normal state and an improvement for the participant. The harmonious convergence of these tripartite metrics, collectively manifesting as improved head and neck control on the tenth day relative to the first day, underscores the robust and enduring efficacy of the visual feedback modality deployed in this study. This empirical exploration unequivocally demonstrates that, following a sequence of ten visual feedback sessions, substantive alterations were observed in the mitigation of maximum head angle deviation, the amelioration of average head angle deviation, and the contraction of the effective range of head angle deviation. In the domain

of policy control by the central nervous system, as quantified by the characteristic of the DFA number, no discernible alteration was ascertained across diverse sessions.

The divergence between post- and pre-visual feedback on the first day was conspicuously substantial, signifying the immediate benefits accrued during the visual feedback sessions. This divergence progressively diminished over time, elucidating the incremental acquisition of skills for maintaining proper head positioning. In the final phases of the learning process, the visual feedback effect displayed a notably reduced positive value, aligning with theoretical expectations, wherein the visual feedback effect asymptotically approaches zero with extended learning. An intrinsic advantage of the developed device lies in its inherent versatility, as it is capable of operation on any standard computer without the need for supplementary equipment. The accelerometer sensor, an integral component of the device, faithfully emulates head movements, offering an efficacious avenue for guiding correct posture. Recent market entries featuring commercial headsets equipped with accelerometers and motion detection capabilities closely approximate the sensor employed in this research, meaning that it can be seamlessly incorporated into commercial products.

Drawing inspiration from this study, there is potential to create wearable sensors equipped with 3D accelerometers to monitor and enhance balance control. These sensors could offer visual feedback to aid elderly individuals or patients with neuromotor disease in improving their balance control.

An inherent limitation of the method resides in the requirement for direct gaze upon the monitor screen, precluding simultaneous engagement in other activities during testing, which could be a potential source of fatigue and reduced concentration. In prospective research endeavors, the incorporation of audio warnings could supplant visual monitoring, affording individuals the freedom to engage in their preferred activities while using the computer, with timely audio cues signaling any departure from optimal head positioning.

Another limitation of this study is the exclusive inclusion of female participants within a restricted age range. Additionally, the absence of follow-up sessions to track the treatment's continued impact after the end of visual feedback represents another constraint.

An accurate comparison between the cost of the proposed design and existing products proves challenging due to several factors. These include the presence of distinct elements and components, as well as the differing levels of confidence perceived by users. The proposed design primarily serves as a prototype aimed at materializing the concept into a small and affordable solution specifically tailored for research purposes. As such, this design is positioned as a cost-effective device concerning a number of elements, such as sensor and controller, which are available with an affordable price, and the simple program, which was already converted into Python language to reduce the cost of the Matlab software.

Envisioning the future, these metrics could be transmitted to specialized centers via internet connectivity, obviating the need for patients to bear travel expenses and reducing the demand on specialists' time. Consequently, this holds the potential to curtail the overall cost of treatment, constituting a promising avenue for the advancement of healthcare delivery. An additional proposal within this domain pertains to the ubiquity of contemporary smartphones, all of which are endowed with sophisticated motion sensors. These cutting-edge motion sensors, integral components of today's smartphones, proffer a compelling opportunity for the creation of a visual feedback system designed to discern and analyze precise user movements. This system can be ingeniously devised to provide instantaneous real-time audio visual feedback to the user should such guidance be deemed requisite. Such an initiative would leverage the existing technological infrastructure of smartphones to foster a novel paradigm in user-directed visual feedback, thereby harnessing the vast potential of mobile devices in the realm of healthcare and self-improvement.

For future endeavors, it is crucial to track the long term impact of visual feedback. Additionally, exploring the option of delivering 3D auditory feedback through a headset could be beneficial. Headsets equipped with sensors to monitor head position could offer a

potential solution akin to other wearable devices, helping to prevent head positions that might lead to health issues.

Author Contributions: Conceptualization: M.E.A.; Methodology: M.E.A.; Validation: M.E.A. and A.J.M.; Investigation: M.E.A., A.J.M. and B.L.; Data curation: M.E.A., A.J.M. and B.L.; Writing—original draft: M.E.A., A.J.M. and B.L.; Writing—review and editing: M.E.A. and A.J.M.; Visualization: M.E.A. and A.J.M.; Administration: M.E.A. and A.J.M.; Supervision: M.E.A.; Project administration: M.E.A., A.J.M. and B.L.; Funding acquisition: M.E.A. and A.J.M. All authors have read and agreed to the published version of the manuscript.

Funding: This work was supported by Jiangxi University of Science and Technology, 341000, Ganzhou, China, under funding number 2021205200100563.

Institutional Review Board Statement: Not applicable.

Informed Consent Statement: Not applicable.

Data Availability Statement: The data are available upon the request.

Acknowledgments: The authors would like to thank RARL (Robotic Automation Reserach Lab, School of Information Engineering, Jiangxi University of Science and Technology, No. 86, Hongqi Ave., Ganzhou 341000, China.

Conflicts of Interest: The authors declare no conflicts of interest.

References

1. Yip, C.H.T.; Chiu, T.T.W.; Poon, A.T.K. The relationship between head posture and severity and disability of patients with neck pain. *Man. Ther.* **2008**, *13*, 148–154. [CrossRef]
2. Chansirinukor, W.; Wilson, D.; Grimmer, K.; Dansie, B. Effects of backpacks on students: Measurement of cervical and shoulder posture. *Aust. J. Physiother.* **2001**, *47*, 110–116. [CrossRef]
3. Kang, J.H.; Park, R.Y.; Lee, S.J.; Kim, J.Y.; Yoon, S.R.; Jung, K.I. The effect of the forward head posture on postural balance in long time computer based worker. *Ann. Rehabil. Med.* **2012**, *36*, 98–104. [CrossRef]
4. Kullgren, A.; Krafft, M.; Nygren, Å.; Tingvall, C. Neck injuries in frontal impacts: Influence of crash pulse characteristics on injury risk. *Accid. Anal. Prev.* **2000**, *32*, 197–205. [CrossRef]
5. Daneshmandi, H.; Majalan, A.S.; Babakhani, M. The comparison of head and neck alignment in children with visual and hearing impairments and its relation with anthropometrical dimensions. *Phys. Treat.* **2014**, *4*, 69–76.
6. Guevara, C.; Jadán-Guerrero, J.; Bonilla-Jurado, D.; Salvador-Ullauri, L.; Acosta-Vargas, P.; Calle-Jimenez, T.; Lara-Alvarez, P. Fuzzy Model for Back Posture Correction During the Walk. In Proceedings of the International Conference on Applied Human Factors and Ergonomics, Washington, DC, USA, 24–28 July 2019; Springer: Cham, Switzerland, 2019; pp. 299–305.
7. Han, G.H.; Yi, C.H.; Kim, S.H.; Kim, S.B.; Lim, O.B. Test–retest Reliability and Concurrent Validity of a Headphone and Necklace Posture Correction System Developed for Office Workers. *Phys. Ther. Korea* **2023**, *30*, 174–183. [CrossRef]
8. Mahmoud, N.F.; Hassan, K.A.; Abdelmajeed, S.F.; Moustafa, I.M.; Silva, A.G. The relationship between forward head posture and neck pain: A systematic review and meta-analysis. *Curr. Rev. Musculoskelet. Med.* **2019**, *12*, 562–577. [CrossRef]
9. Fernández-de-Las-Peñas, C.; Cuadrado, M.L.; Pareja, J.A. Myofascial trigger points, neck mobility and forward head posture in unilateral migraine. *Cephalalgia* **2006**, *26*, 1061–1070. [CrossRef]
10. Ruivo, R.M.; Pezarat-Correia, P.; Carita, A.I. Effects of a resistance and stretching training program on forward head and protracted shoulder posture in adolescents. *J. Manip. Physiol. Ther.* **2017**, *40*, 1–10. [CrossRef]
11. Cole, A.K.; McGrath, M.L.; Harrington, S.E.; Padua, D.A.; Rucinski, T.J.; Prentice, W.E. Scapular bracing and alteration of posture and muscle activity in overhead athletes with poor posture. *J. Athl. Train.* **2013**, *48*, 12–24. [CrossRef] [PubMed]
12. Avery, R.M. Massage therapy for cervical degenerative disc disease: Alleviating a pain in the neck? *Int. J. Ther. Massage Bodyw.* **2012**, *5*, 41.
13. Kim, D.; Cho, M.; Park, Y.; Yang, Y. Effect of an exercise program for posture correction on musculoskeletal pain. *J. Phys. Ther. Sci.* **2015**, *27*, 1791–1794. [CrossRef] [PubMed]
14. Abdollahzade, Z.; Shadmehr, A.; Malmir, K.; Ghotbi, N. Effects of 4 week postural corrective exercise on correcting forward head posture. *J. Mod. Rehabil.* **2017**, *11*, 85–92.
15. Frank, D.L.; Khorshid, L.; Kiffer, J.F.; Moravec, C.S.; McKee, M.G. Biofeedback in medicine: Who, when, why and how? *Ment. Health Fam. Med.* **2010**, *7*, 85.
16. Mohamed, A.A.; Jan, Y.K.; Raoof, N.A.; Kattabei, O.; Moustafa, I.; Hosny, H. Effect of biofeedback corrective exercise on reaction time and central somatosensory conduction time in patients with forward head posture and radiculopathy: A randomized controlled study. *J. Chiropr. Med.* **2022**, *21*, 39–50. [CrossRef] [PubMed]
17. Peper, E.; Shaffer, F. Biofeedback history: An alternative view. *Biofeedback* **2018**, *46*, 80–85. [CrossRef]

18. Afzal, M.R.; Oh, M.K.; Yoon, J. Development of a multimodal biofeedback system for balance training. In Proceedings of the IEEE International Conference of Advanced Intelligent Mechatronics (AIM), Busan, Republic of Korea, 7–11 July 2015; pp. 658–663.
19. Al Osman, H.; Eid, M.; El Saddik, A. U-biofeedback: A multimedia-based reference model for ubiquitous biofeedback systems. *Multimed. Tools Appl.* **2014**, *72*, 3143–3168. [CrossRef]
20. Giggins, O.M.; Persson, U.M.; Caulfield, B. Biofeedback in rehabilitation. *J. Neuro Eng. Rehabil.* **2013**, *10*, 60. [CrossRef]
21. Tsai, P.S.; Chang, N.C.; Chang, W.Y.; Lee, P.H.; Wang, M.Y. Blood pressure biofeedback exerts intermediate-term effects on blood pressure and pressure reactivity in individuals with mild hypertension:a randomized controlled study. *J. Altern. Complement. Med.* **2007**, *13*, 547–554. [CrossRef] [PubMed]
22. Patel, C.; Datey, K.K. Relaxation and biofeedback techniques in the management of hypertension. *Angiology* **1976**, *27*, 106–113. [CrossRef]
23. Joshi, S.; Chawla, B.; Pawalia, A. Exercises in the management of forward head posture: Much needed posture care for online way of life. *Physiother. Q.* **2022**, *30*, 41–51. [CrossRef]
24. Lee, K.J.; Oh, J.S.; Kim, S.G. Effect of Biomechanical Feedback Device Utilizing Tilt and Tension Sensors on Young Adults Balance Control Ability, Proprioception and Craniovertebral Angle (CVA). *J. Reatt. Ther. Dev. Divers.* **2023**, *6*, 526–534.
25. Breen, P.P.; Nisar, A.; ÓLaighin, G. Evaluation of a single accelerometer based biofeedback system for real-time correction of neck posture in computer users. In Proceedings of the 2009 Annual International Conference of the IEEE Engineering in Medicine and Biology Society, Minneapolis, MN, USA, 3–6 September 2009; pp. 7269–7272.
26. Lee, J.; Cho, E.; Kim, M.; Yoon, Y.; Choi, S. PreventFHP: Detection and warning system for forward head posture. In Proceedings of the 2014 IEEE Haptics Symposium (HAPTICS), Houston, TX, USA, 23–26 February 2014; pp. 295–298.
27. Liao, D.Y. Design of a secure, biofeedback, head-and-neck posture correction system. In Proceedings of the 2016 IEEE First International Conference on Connected Health: Applications, Systems and Engineering Technologies (CHASE), Washington, DC, USA, 27–29 June 2016; pp. 119–124.
28. Oh, H.J.; Song, G.B. Effects of neuro feedback training on the cervical movement of adults with forward head posture. *J. Phys. Ther. Sci.* **2016**, *28*, 2894–2897. [CrossRef]
29. Kuo, Y.L.; Wang, P.S.; Ko, P.Y.; Huang, K.Y.; Tsai, Y.J. Immediate effects of real-time postural biofeedback on spinal posture, muscle activity, and perceived pain severity in adults with neck pain. *Gait Posture* **2019**, *67*, 187–193. [CrossRef] [PubMed]
30. Andani, M.E.; Salehi, Z. An affordable and easy-to-use tool to diagnose knee arthritis using knee sound. *Biomed. Signal Process. Control* **2024**, *88*, 105685. [CrossRef]
31. Alcan, V.; Zinnuroğlu, M. Current developments in surface electromyography. *Turk. J. Med. Sci.* **2023**, *53*, 1019–1031. [CrossRef]
32. Thurzo, A.; Strunga, M.; Havlínová, R.; Reháková, K.; Urban, R.; Surovková, J.; Kurilová, V. Smartphone-Based Facial Scanning A Viable Tool Facially Driven Orthodontics? *Sensors* **2022**, *12*, 7752. [CrossRef] [PubMed]
33. Ko, M.J.; Koo, M.S.; Jung, E.J.; Jeong, W.J.; Oh, J.S. Effect of Pelvic Floor Muscle Training Using Pressure Biofeedback on Pelvic Floor Muscle Contraction and Trunk Muscle Activity in Sitting in Healthy Women. *Healthcare* **2022**, *10*, 570. [CrossRef] [PubMed]
34. Cesari, P.; Cristani, M.; Demrozi, F.; Pascucci, F.; Picotti, P.M.; Pravadelli, G.; Zenti, L. Towards Posture and Gait Evaluation through Wearable-Based Biofeedback Technologies. *Electronics* **2023**, *12*, 644. [CrossRef]
35. Hribernik, M.; Umek, A.; Tomažič, S.; Kos, A. Review of real-time biomechanical feedback systems in sport and rehabilitation. *Sensors* **2022**, *22*, 3006. [CrossRef]
36. Kibushi, B.; Okada, J. Auditory sEMG biofeedback for reducing muscle co-contraction during pedaling. *Physiol. Rep.* **2022**, *10*, e15288. [CrossRef]
37. Toledo-Peral, C.L.; Vega-Martínez, G.; Mercado-Gutiérrez, J.A.; Rodríguez-Reyes, G.; Vera-Hernández, A.; Leija-Salas, L.; Gutiérrez-Martínez, J. Virtual/Augmented reality for rehabilitation applications using electromyography as control/biofeedback: Systematic literature review. *Electronics* **2022**, *11*, 2271. [CrossRef]
38. Baer, J.L.; Vasavada, A.; Cohen, R.G. Posture biofeedback increases cognitive load. *Psychol. Res.* **2022**, *86*, 1892–1903. [CrossRef]
39. Moshayedi, A.J.; Hosseinzadeh, M.; Joshi, B.P.; Emadi Andani, M. Recognition System for Ergonomic Mattress and Pillow: Design and Fabrication. *IETE J. Res.* **2023**, 1–19. [CrossRef]
40. Moshayedi, A.J.; Uddin, N.M.I.; Khan, A.S.; Zhu, J.; Emadi Andani, M. Designing and Developing a Vision-Based System to Investigate the Emotional Effects of News on Short Sleep at Noon: An Experimental Case Study. *Sensors* **2023**, *23*, 8422. [CrossRef]
41. Faul, F.; Erdfelder, E.; Lang, A. G.; Buchner, A. G* Power 3: A flexible statistical power analysis program for the social, behavioral, and biomedical sciences. *Behav. Res. Methods* **2007**, *39*, 175–191. [CrossRef] [PubMed]
42. Cohen, J. *Statistical Power Analysis for the Behavioral Sciences*, 2nd ed.; Lawrence Erlbaum Associates: Hillsdale, NJ, USA, 1988.
43. Emadi Andani, M.; Villa-Sánchez, B.; Raneri, F.; Dametto, S.; Tinazzi, M.; Fiorio, M. Cathodal cerebellar tDCS combined with visual feedback improves balance control. *Cerebellum* **2020**, *19*, 812–823. [CrossRef] [PubMed]
44. Moshayedi, A.J.; Sambo, S.K.; Kolahdooz, A. Design and development of cost-effective Exergames for activity incrementation. In Proceedings of the 2022 2nd International Conference on Consumer Electronics and Computer Engineering (ICCECE), Guangzhou, China, 14–16 January 2022. [CrossRef]
45. Cueva, J.H.; Castillo, D.; Espinós-Morató, H.; Durán, D.; Díaz, P.; Lakshminarayanan, V. Detection and classification of knee osteoarthritis. *Diagnostics* **2022**, *1*, 2362. [CrossRef]
46. Hausdorff, J.M.; Peng, C.K.; Ladin, Z.V.I.; Wei, J.Y.; Goldberger, A.L. Is walking a random walk? Evidence for long-range correlations in stride interval of human gait. *J. Appl. Physiol.* **1995**, *78*, 349–358. [CrossRef] [PubMed]

47. Peng, C.K.; Mietus, J.; Hausdorff, J.M.; Havlin, S.; Stanley, H.E.; Goldberger, A.L. Long-range anticorrelations and non-Gaussian behavior of the heartbeat. *Phys. Rev. Lett.* **1993**, *70*, 1343. [CrossRef] [PubMed]
48. Terrier, P.; Deriaz, O. Kinematic variability, fractal dynamics and local dynamic stability of treadmill walking. *J. Neuroeng. Rehabil.* **2011**, *8*, 12. [CrossRef] [PubMed]
49. Hausdorff, J.M.; Schaafsma, J.D.; Balash, Y.; Bartels, A.L.; Gurevich, T.; Giladi, N. Impaired regulation of stride variability in Parkinson's disease subjects with freezing of gait. *Exp. Brain Res.* **2003**, *149*, 187–194. [CrossRef] [PubMed]